Published in: Prostaglandins & Other Lipid Mediators (2006), vol.79, iss.1-2, pp.53-73
Status: Postprint (Author's version)

Evaluation of BM-573, a novel TXA_2 synthase inhibitor and receptor antagonist, in a porcine model of myocardial ischemia-reperfusion

Philippe Kolh[a,1], Stéphanie Rolin[b,1], Vincent Tchana-Sato[a], Michel Pétein[c], Alexandre Ghuysen[a], Bernard Lambermont[a], Julien Hanson[d], David Magis[e], Patrick Segers[f], Bernard Masereel[b], Vincent D'Orio[a], Jean-Michel Dogne[b]

[a] *Hemodynamic Research Center (HemoLiège), University of Liège, Belgium*

[b] *Department of Pharmacy, University of Namur, Belgium*

[c] *Institute of Pathology and Genetics, Loverval, Belgium*

[d] *Natural and Synthetic Drugs Research Center, University of Liège, Belgium*

[e] *Department of Biostatistics, University of Liège, Belgium*

[f] *Hydraulics Laboratory, Institute Biomedical Technology, Ghent University, Belgium*

Abstract

Aims: To investigate whether BM-573 (*N-tert*-butyl-*N'*-[2-(4'-methylphenylamino)-5-nitro-benzenesulfonyl]urea), an original combined thromboxane A_2 synthase inhibitor and receptor antagonist, prevents reperfusion injury in acutely ischemic pigs. *Methods:* Twelve animals were randomly divided in two groups: a control group (n = 6) intravenously infused with vehicle, and a BM-573-treated group (n = 6) infused with BM-573 (10 $mgkg^{-1}$ h^{-1}). In both groups, the left anterior descending (LAD) coronary artery was occluded for 60 min and reperfused for 240 min. Either vehicle or BM-573 was infused 30 min before LAD occlusion and throughout the experiment. Platelet aggregation induced by arachidonic acid ex vivo measured was prevented by BM-573. *Results:* In both groups, LAD occlusion decreased cardiac output, ejection fraction, slope of stroke work—end-diastolic volume relationship, and induced end-systolic pressure-volume relationship (ESPVR) rightward shift, while left ventricular afterload increased. Ventriculo-arterial coupling and mechanical efficiency decreased. In both groups, reperfusion further decreased cardiac output and ejection fraction, while ESPVR displayed a further rightward shift. Ventriculo-arterial coupling and mechanical efficiency remained impaired. Area at risk, evidenced with Evans blue, was 33.2 ± 3.4% of the LV mass (LVM) in both groups, and mean infarct size, revealed by triphenyltetrazolium chloride (TTC), was 27.3 ± 2.6% of the LVM in the BM-573-treated group (NS). Histological examination and immunohistochemical identification of desmin revealed necrosis in the anteroseptal region similar in both groups, while myocardial ATP dosages and electron microscopy also showed that BM-573 had no cardioprotective effect. *Conclusions:* These data suggest that BM-573 failed to prevent reperfusion injury in acutely ischemic pigs.

Keywords: Thromboxane synthase inhibitor; Thromboxane receptor antagonist; Myocardial ischemia; Reperfusion injury; Contractile function; Hemodynamics; Pig

1. Introduction

Myocardial ischemia in the clinical setting is usually a consequence of a thrombotic occlusion of a coronary artery at the site of a ruptured atherosclerotic plaque. Prompt re-establishment of coronary flow following coronary occlusion is mandatory for the preservation of myocardial tissue. The establishment of reperfusion, originally by coronary thrombolysis and subsequently also by percutaneous coronary interventions, was a major improvement in the management of patients with myocardial infarction and rapidly gained wide acceptance [1-3].

A short a time as possible between coronary occlusion and reperfusion is mandatory for successful salvage of myocardial tissue, so as to decrease post-myocardial infarction mortality [4]. However, paradoxically,

[1] Both authors have equally contributed to this work.

myocardial damage is still observed even after early successful reperfusion. This and other observations led to the concept that, although reperfusion is needed for myocardial salvage, it may also trigger a further series of harmful events which add to myocardial injury. That part of myocardial injury and the clinical manifestations specifically triggered by reperfusion have been labelled "ischemia reperfusion-induced injury" [5,6]. It has been suggested that the impact of reperfusion plays a key role in accelerating the expression of irreversible myocardial damage caused by ischemia.

Many factors contribute to the reperfusion injury characterised by cell death which not only occurs through necrosis. Generation of reactive oxygen species, including the superoxide anion, hydrogen peroxide and hydroxyl radicals are involved since they would trigger cardiac cell death through apoptotic mechanisms [7]. Intra-cellular calcium overload, accumulation, activation and infiltration of neutrophils releasing lysosomial enzymes and arachidonic acid products, endothelial dysfunction leading to a compromised microvascular nutritional blood flow (the "no-reflow" phenomenon) and activation of the renin-angiotensin system are other possibilities [8-10]. Some of these mechanisms are possibly interrelated and act together in the creation of reperfusion injury. On the basis of the possible multiple physiological mechanisms that are involved, a large number of pharmacological agents have been studied with the overall objective of reducing final infarct size. Among compounds tested are hydroxyl radical scavengers, antioxidants, beta-blockers, calcium antagonists, inhibitors of the renin-angiotensin system, and thromboxane receptors antagonists.

It is well established that thromboxane A_2 (TXA_2), abnormally released during myocardial ischemia and reperfusion, in humans [11,12] and in animal models [13-15], mediates several pathophysiological states and events due to its biological activities as platelet aggregation, constriction of vascular smooth muscles, leukocyte chemotaxis, smooth muscle cells proliferation,…Consequently, blockade of TXA_2 receptor with antagonists and/or inhibit TXA_2 synthase with specific inhibitors could protect cardiac cells against deleterious effects of ischemia, but this remains a matter of debate as several studies have yielded contradictory results for TXA_2 receptor antagonists. Indeed, it has been demonstrated that such compounds were able to reduce the severity of myocardial infarction [15,16], while other studies failed to observe such protective effects [17,18].

Therefore, the aim of the present work was to determine whether BM-573 (*N*-tertbutyl-*N'*-[2-(4'-methylphenylamino)-5-nitro-benzenesulfonyl]urea), an original non-carboxylic combined TXA_2 synthase inhibitor and TXA_2 receptor antagonist [19-21], would be able to prevent or to decrease ischemia-reperfusion injury in pigs suffering from 60 min ischemia followed by 240 min of reperfusion. Hemodynamic, histopathological, biochemical, and aggregrometric parameters were thoroughly evaluated.

2. Materials and methods

2.1. Preparation

All experimental procedures and protocols used in this investigation were reviewed and approved by the Ethics Committee of the Medical Faculty of the University of Liège. All procedures conformed to the *Guiding Principles in the Care and Use of Animals* of the American Physiological Society and were performed according to the *Guide for the Care and Use of Laboratory Animals*, [NIH publication no. 85-23, revised 1996].

Experiments were performed on 12 healthy pure pietran pigs of either sex (20-28 kg). The animals were premedicated with intramuscular administration of ketamine (20 mg kg^{-1}) and diazepam (1 mg kg^{-1}). Anesthesia was then induced and maintained by a continuous infusion of sufentanil (0.5 µg kg^{-1} h^{-1}) and sodium pentobarbital (3 mg kg^{-1} h^{-1}). Spontaneous movements were prevented by pancuronium bromide (0.1 mg kg^{-1} h^{-1}). After endotracheal intubation through a cervical tracheostomy, the pigs were connected to a volume-cycled ventilator (Evita 2, Dräger, Lübeck, Germany) set to deliver a tidal volume of 15 ml kg^{-1} at a respiratory rate of 20 min^{-1}. End-tidal pCO_2 measurements (Capnomac, Datex, Helsinki, Finland) were used to monitor the adequacy of ventilation. Respiratory settings were adjusted to maintain end-tidal pCO2 in the range of 35-40 Torr (4.67-5.33 kPa). Arterial oxygen saturation was closely monitored and maintained above 95% by adjusting the FiO_2 as necessary. Central temperature was measured with a rectal probe and maintained at 37 °C by means of a heating blanket. A standard lead electrocardiogram was used for the monitoring of heart rate (HR).

The chest was entered through median sternotomy, the pericardium was incised and sutured to the chest wall to form a cradle for the heart, and the root of the aorta was dissected clear of adherent fat and connective tissue. A combined conductance-micromanometer catheter (CD Leycom, Zoetermeer, The Netherlands) was inserted through the right carotid artery and advanced into the left ventricle. A micromanometer-tipped catheter (Sentron pressure measuring catheter, Cordis, Miami, FL, USA) was inserted through the right femoral artery and

advanced into the ascending aorta. A 14 mm diameter perivascular flow-probe (Transonic Systems Inc., Ithaca, NY, USA) was closely adjusted around the aorta 2 cm downstream to the aortic valve. The micromanometer-tipped catheter was manipulated so that the pressure sensor was positioned just distal to the flow probe. Right atrial pressure was measured with a micromanometer-tipped catheter inserted into the cavity through the superior vena cava. A 6F Fogarty balloon catheter (Baxter Healthcare Corp., Oakland, CA, USA) was advanced into the inferior vena cava through a right femoral venotomy. Inflation of this balloon produced a titrable leftward shift in pressure-volume loops by reducing venous return. The jugular vein and the left femoral artery were cannulated for eventual drug administration and for blood samples analysis, respectively.

A segment of the left anterior descending (LAD) coronary artery was isolated distal to the first diagonal branch for later application of a surgical clamp. An ultrasonic flow probe (Transonic Systems Inc., Ithaca, NY, USA) was placed around the LAD coronary artery three centimetres distal to the site of planned occlusion, to measure coronary artery blood flow.

2.2. Hemodynamic measures

To provide similar states of vascular filling, the animals were continuously infused with Ringer lactate (5 ml kg^{-1} h^{-1}), and, when necessary, with hydroxyethylstarch 6% to increase central venous pressure up to 6-7 mmHg over 30 min. Baseline hemodynamic recordings were obtained thereafter including simultaneous measurements of aortic pressure and flow waveforms necessary to identify parameters of the three-element windkessel model. A first diagram of the left ventricular pressure-volume relationship was generated from volume and pressure measurements at baseline and during gradual decreases in preload by reducing venous return. The caval occlusion was limited to a few seconds in duration in order to avoid reflex responses. All measurements were taken immediately after the animal was briefly disconnected from the ventilator to sustain end-expiration. After deflation of the inferior vena cava balloon, the animals were allowed to rest for an additional 30 min.

The animals were then randomly divided in two groups: a control group (n = 6) intravenously infused with vehicle (propylene glycol-NaCl 0.9%, 50:50), and a BM-573-treated group (n = 6) infused with BM-573 (10 mg kg^{-1} h^{-1}). The animals were then followed for 30 min, and hemodynamic measures were again obtained. Thereafter, the LAD coronary artery was occluded at the site of previous dissection. The occlusion was maintained for 60 min, period after which the LAD coronary artery was reperfused for 240 min in both groups. In all animals, hemodynamic measurements were obtained every 30 min throughout the experiment. Either vehicle or BM-573 was infused until the end of the experiment.

2.2.1. Data collection

The conductance catheter was connected to a Sigma-5 signal-conditioner processor (CD Leycom, Zoetermeer, The Netherlands). Each ultrasonic flow-probe was connected to a flow-meter (HT 207, Transonic Systems Inc., Ithaca, NY, USA), and each micromanometer-tipped catheter to the appropriate monitor (Sentron pressure monitoring, Cordis, Miami, FL, USA). All analog signals and the ventricular pressure-volume loops were displayed on screen for continuous monitoring. The analog signals were continuously converted to digital form with an appropriate software (Codas, DataQ Instruments Inc., Akron, OH, USA) at a sampling frequency of 200 Hz.

2.2.2. Data analysis

2.2.2.1. Ventricular systolic function. Left ventricular volumes were inferred using the dual field conductance catheter technique [22]. Calibration of the conductance signal to obtain absolute volume was performed by the hypertonic saline method [22]. Therefore, a small volume (1-2 ml) of 10% NaCl solution was injected into the pulmonary artery during continuous data acquisition.

LV contractile function was assessed by the end-systolic pressure-volume relation (ESPVR), and the preload recruitable stroke work (PRSW).

The instantaneous pressure-volume relationship was considered in terms of a time-varying elastance $E\{t\}$, defined by the following relationship:

$$E(t) = \frac{P(t)}{[V(t) - V_{\mathrm{d}}]}$$

where *P(t)* and *V(t)* are, respectively, the instantaneous ventricular pressure and volume, and V_d a correction term. End-systole was defined as the instant of time in the ejection phase at which *E(t)* reaches its maximum, E_{max}. It has been demonstrated that *E(t)* and V_d are insensitive to preload, at least within physiological ranges [23]. Preload was acutely reduced by inflating the inferior vena cava balloon catheter.

Stroke work (SW) was calculated as the area enclosed within each pressure-volume loop and was plotted against end-diastolic volume (EDV; volume at the lower right corner of the loop) to generate the SW-EDV relation (preload recruitable stroke work, PRSW).

2.2.2.2. Myocardial energetics. Myocardial energetics was assessed by computation of pressure-volume area (PVA). In the time-varying elastance model of the ventricle, the total energy generated by each contraction is represented by the total area under the end-systolic pressure-volume relation line and the systolic segment of the pressure-volume loop, and above the end-diastolic pressure volume relation curve, and denoted by PVA (Fig. 3) [24]. PVA is the sum of SW (the energy that the ventricle delivers to the blood at ejection) and potential energy (PE; necessary to overcome the viscoelastic properties of the myocardium itself). It has been demonstrated that PVA was highly correlated with myocardial oxygen consumption [25].

Mechanical efficiency was defined as the SW/PVA ratio.

2.2.2.3. Arterial properties. Arterial properties were assessed from ascending aortic pressure and flow measurements and represented with a three-element windkessel model (WK3) [26]. In this model, the resistor R_2 represents the resistive properties of the systemic bed, which are considered to reside primarily in the arteriolar system. The capacitor C, placed in parallel with R_2, represents the compliant properties of the large systemic arteries. The resistor R_1 represents the characteristic impedance, which level depends prominently on the elastic properties of the proximal aorta.

The values of R_1, R_2, and C were estimated by a method previously described [27]. Effective arterial elastance (E_a) was calculated according to the equation [28]:

$$E_a = \frac{R_1 + R_2}{T_s + R_2 C(1 - e^{-T_d/R_2 C})}$$

where T_s and T_d are the systolic and diastolic time intervals, respectively. T_s was calculated, in the aortic pressure wave, as the time interval between the point just before the abrupt rise and the dicrotic notch. Ventriculo-arterial coupling was appreciated through the ratio E_{es}/E_a.

2.3. Area at risk and infarct size quantifications

Risk area and infarct area were delineated by a dual staining technique [20,29,30]. Immediately before the end of the experiment, 20 ml of Evans blue dye solution (0.1 g ml^{-1} in 50 mM phosphate buffered saline, pH 7.4) were injected into the jugular vein, to stain the non-ischemic area blue. The pig was then sacrificed with an intravenous injection of pentobarbital (100 mg kg^{-1}). The heart was then rapidly harvested, rinsed with a cold isotonic saline solution and sectioned in five transverse slices (0.6 cm thick) from apex to base (S1-S5). The LV risk area, due to its anatomical dependence on the LAD coronary artery for blood flow, was identified in the anteroseptal region by lack of Evans blue in this region.

Gross slices were photographed with a digital camera (Fujifilm FinePix 2400 Zoom). Morphological changes in size, shape and transmural distribution of myocardial infarction were measured using 2,3,5-triphenyltetrazolium chloride (TTC) staining (Sigma-Aldrich Chemical Co., St. Louis, MO, USA). Tissue slices were rinsed with a cold isotonic saline solution and then incubated at 38 °C for 15-20 min in a phosphate-buffered solution of TTC (1% in 0.1 M, pH 7.4) [31,32]. This produced a brick red coloration in the presence of dehydrogenase enzymes in intact myocardium whereas infracted regions remained unstained due to the collapse of enzyme activity. After photography with a digital camera (Fujifilm FinePix 2400 Zoom, Elmsford, NY, USA), slices of myocardium were placed in 10% neutral-buffered formaldehyde to enhance the contrast between stained and unstained regions. After 3 days of fixation in formalin and just before paraffin proceeding, myocardial sections were again photographed with a video camera (3CCD color video, DXC-390P ExwaveHAD, Sony, New York, NY, USA). Infarct size was measured from the tracings of these photographed myocardial slices to a clear acetate sheet and the area of each zone was then weighted. The ratio between the two zones (ischemic area and non-ischemic area) was determined for each slice.

Infarct size measured from the tracings of myocardial slices was calculated by planimetry as a percentage of LV mass.

2.4. Histopathogical analysis of myocardium

After 3 days, three or four tissue-blocks were taken from each slice at standardised locations and routinely processed for paraffin histology. The tissue blocks from myocardium were cut at 6 µm and each section was stained with hematoxylin and eosin (H&E) and Masson trichrome stain. The stained sections were examined at magnifications of x25, x100, x200 and x400 to study the distribution of infarction. Photomicrographs were taken using a Zeiss photomicroscope (Axioscope 2 plus-Sony 3CCD camera, 1024-768 pixels definition, Thornwood, NY, USA). In addition, all tissue-blocks of slice S3 were processed for immunohistochemical staining of desmin to investigate more in details cardiac muscle's lesions. Monoclonal antibodies to desmin (clone D33, Biomeda, Foster City, CA, USA) were diluted 1/20.

2.5. Electron microscopy

Samples from cardiac tissue (2-3 mm square and 1 mm thick) were taken from anteroseptal and posterior regions of slice S2 and were kept in freshly prepared glutaraldehyde buffer fixative. Tissue samples were embedded in Epon after fixation in 2% osmium tetroxide, dehydration in ethanol series and substitution by propylene oxide. Semi-thin sections (2 µM) were cut, mounted on glass microscope slides and stained with toluidine blue. After examination of the semi-thin sections by light microscopy, artifact-free areas were selected for preparation of thin sections (90 nm) for electron microscopy. These sections were coated on copper grids, stained with uranyl acetate and viewed in a JEOL 1200 EXII transmission electron microscope (JEOL, Tokyo, Japan). For each sample, 15-20 micrographs were examined to characterise cardiomyocytes injury.

2.6. Biochemical markers dosages (Cardiac myocytes ATP, plasmatic creatine phosphokinase and plasmatic troponine T levels)

The myocardial ATP content was measured by an adaptation of the ATP bioluminescent assay kit (Sigma-Aldrich diagnostic kit, St. Louis, MO, USA). There is a linear relationship between the relative light intensity generated by luciferin-luciferase reaction and the ATP concentration. Samples of cardiac tissue taken from anteroseptal and posterior regions of slice S2 were sequentially frozen in liquid nitrogen and then conserved at -80 °C till ATP dosage. Sample was mechanically disrupted, reduced in powder and then suspended in 700 µl of somatic cell ATP releasing reagent. The suspension was then homogenised with a Dounce (10 times), diluted with ultra pure water and 10 µl added to 100 µl of ATP assay mix (luciferase, luciferin, $MgSO_4$, EDTA, DTT and BSA in a Tricine buffer). For each sample, luminescence in Relative Light Unit (RLU) was determined with a luminometer (LUMAC Biocounter M2010). Bradford's protein dosage was performed, and results expressed in nmol $ATPg^{-1}$ of protein.

Arterial blood samples were taken every 60 min after starting LAD occlusion. Samples were collected in plastic tubes containing 1/10 volume of 3.8% trisodium citrate and were centrifuged at 2205 × *g* for 10 min at 15 °C. The supernatant was removed and analysed for plasma creatine phosphokinase (CPK) and troponine T (TnT) concentrations.

2.7. Ex vivo platelet aggregation study

The antiplatelet potency of BM-573 was determined according to a previously described method [21]. Briefly, blood samples were collected using tubes containing 1:9 citrate (final conc. 0.38%). The platelet-rich plasma (PRP) was obtained from the supernatant fraction after centrifugation for 20 min at 90 × *g* (25 °C). The remaining blood was centrifuged at 1200 × *g* for 10 min (25 °C) and the supernatant gave the platelet-poor plasma (PPP). The platelet concentration of PRP was adjusted to 3×10^8 cells ml^{-1} by dilution with PPP. Aggregation tests were performed according to Born's turbidimetric method by means of a four-channel aggregometer (bioData Corporation, PAP4). PPP was used to adjust the photometric measurement to the minimum optical density. PRP (225 µl) was added in a silanised cuvette and stirred (1100 rev min^{-1}). Platelet aggregation was initiated by addition of (5 µl) arachidonic acid (600 µM final) or (1 µl) U-46619 (1 µM final). To evaluate platelet aggregation, the maximum increase in light transmission (platelet aggregation amplitude) was determined from the aggregation curve 6 min after addition of the inducer.

2.8. Statistical analysis

All data are expressed as mean ± standard error of the mean (S.E.M.). Changes in ventricular and arterial parameters, and offsets for various relationships, were evaluated by a two-way repeated measures analysis of variance, with time as the first factor, and intervention (vehicle/BM573) as the second factor.

When the Snedecor *F* was significant, multiple comparisons were made with the Scheffe test. Results of statistical tests were considered significant for a level of uncertainty of 5% ($P < 0.05$). Statistical tests were performed using the Statistica software (Statsoft Inc, OK, USA).

3. Results

3.1. Hemodynamic data

There was no statistically significant difference between the two groups, at baseline in any of the measured or calculated hemodynamic parameters. At baseline, LAD coronary artery blood flow was 42.3 ± 1.6 ml min^{-1} in the vehicle group, and 41.5 ± 2.4 ml min^{-1} in the BM-573-treated group (NS).

3.1.1. Effects of acute regional ischemia

The evolution during myocardial ischemia was statistically comparable in the two groups for all measured or calculated hemodynamic parameters. In both groups, LAD coronary artery blood flow immediately dropped to zero after application of the surgical clamp.

While mean aortic pressure remained stable, heart rate increased from 102 ±6 beats min^{-1} at baseline to 114 ± 9 beats min^{-1} at T60 ($P = 0.02$) and mean aortic flow decreased from 73.2 ± 4.9 ml s^{-1} at baseline to 62.6 ± 5.8mls^{-1} at T60 ($P = 0.01$) (Fig. 1).

Applying the WK3 model to the aortic pressure and flow waveforms, we observed that peripheral resistance R_2 significantly ($P = 0.01$) increased from 1.34 ± 0.17 mmHg s ml^{-1} to 1.64 ± 0.24 mmHg s ml^{-1}, between baseline and T60 (Fig. 2). In the same interval, neither characteristic impedance R_1 nor compliance C did significantly change. As a consequence, effective arterial elastance E_a, integrating LV afterload, increased from 2.58 ± 0.34 mmHg ml^{-1} to 3.44 ± 0.55 mmHg ml^{-1}, between baseline and T60 ($P = 0.001$).

As represented in Fig. 3, end-systolic volume V_{es} varied from 31.8 ±6.2 ml at baseline to 37.1 ±3.6 ml at T60 ($P = 0.09$), while end-diastolic volume V_{ed} did not change. However, in the same interval, stroke volume SV and ejection fraction EF decreased from 38.9 ± 3.4 ml at baseline to 31.0 ± 1.6 ml at T60 ($P = 0.001$), and from 57 ± 4% at baseline to 46 ± 2% at T60 ($P = 0.005$), respectively.

While end-systolic elastance E_{es} remained unchanged, dead volume V_d increased from -27.7 ± 6.6 ml at baseline to -13.7 ± 3.9 ml at T60 ($P = 0.005$) (Fig. 4). In the same interval, the slope of the preload recruitable stroke work decreased from 76.7 ±6.6 mmHg to 66.4 ± 5.6 mmHg ($P = 0.001$), and left ventriculo-arterial coupling E_{es}/E_a from 0.71 ±0.10 to 0.56 ± 0.11 ($P = 0.01$).

As illustrated in Fig. 5, stroke work SW and pressure-volume area PVA, respectively decreased from 3900 ± 239 mmHg ml to 2829 ± 244 mmHg ml ($P = 0.001$), and from 7033 ± 508 mmHg ml to 5616 ± 606 mmHg ml ($P = 0.01$), between baseline and T60. As a consequence, mechanical efficiency SW/PVA changed, in the same time interval, from 0.55 ± 0.04 to 0.50 ± 0.03 ($P = 0.04$).

3.1.2. Effects of coronary reperfusion

The evolution during myocardial reperfusion was statistically comparable in the two groups for all measured or calculated hemodynamic parameters. Shortly after removal of the surgical clamp, LAD coronary blood flow was measured at 39.6 ± 4.5 ml min^{-1} in the vehicle group, and at 40.9 ± 3.8 ml min^{-1} in the BM-573-treated group (NS between groups and versus baseline). In either group, it did not significantly change thereafter.

In both groups, reperfusion induced a further decrease in mean aortic blood flow (from 62.6 ± 10.8 ml s^{-1} at T60 to 44.6 ± 6.9 ml s^{-1} at T300; $P<0.001$), and an increase in heart rate (from 114 ± 9 beats min^{-1} at T60 to 140 ± 5 beats min^{-1} at T300; $P = 0.003$), while mean aortic pressure did not significantly change (Fig. 1).

Fig. 1: *Evolution of mean aortic pressure P_{mean}, mean aortic flow Q_{mean}, and heart rate HR during myocardial ischemia and reperfusion. Ischemia was induced immediately after baseline recordings (TO) by occluding the LAD coronary artery, which was reperfused after T60 measurements. *P<0.05 vs. T0; **P<0.01 vs. T0; ***P<0.001 vs. T0; ## P<0.01 vs. T60; ### P< 0.001 vs. T60.*

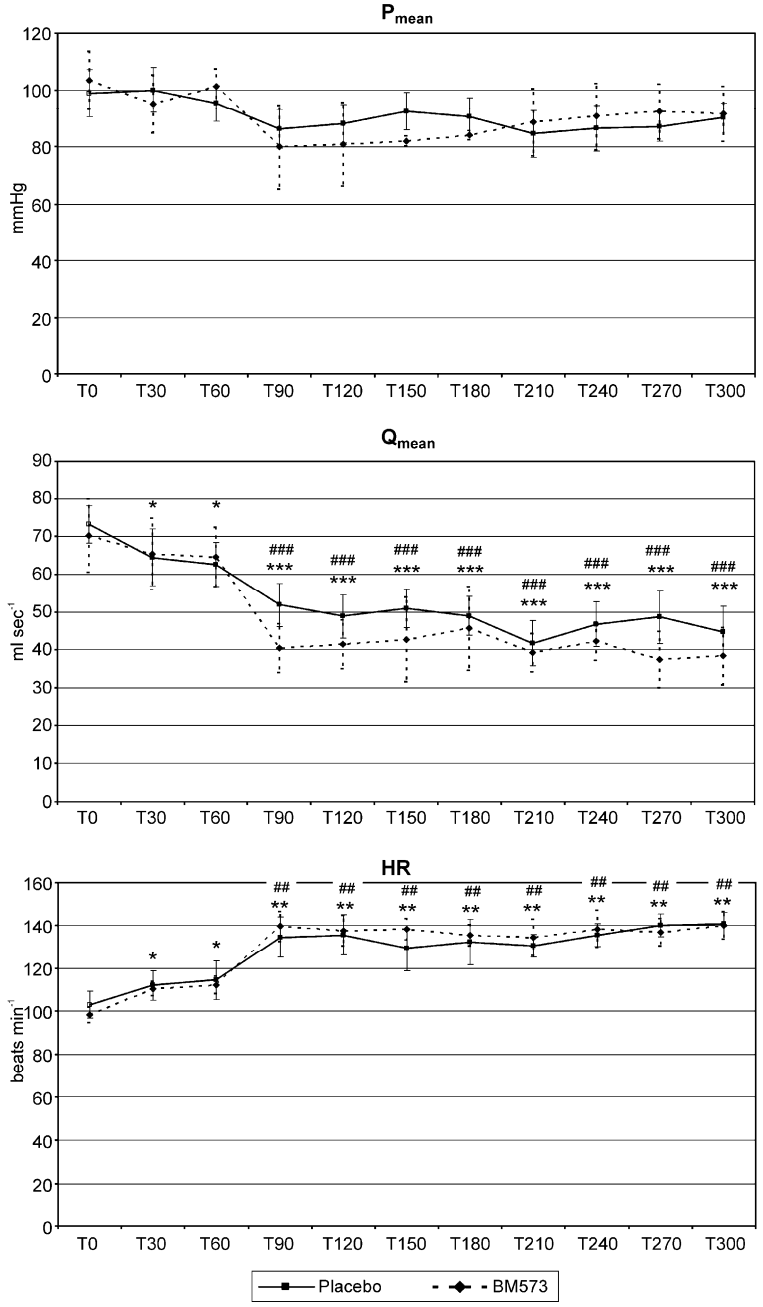

Applying the WK3 model to the aortic pressure and flow waveforms, we observed that, in both groups, characteristic impedance and compliance remained unchanged, while peripheral resistances R_2 increased significantly (P = 0.02) from 1.64 ± 0.24 mmHg s ml^{-1} at T60 to 2.28 ± 0.38 mmHg s ml^{-1} at T300 (Fig. 2). As a consequence, effective arterial elastance increased (P = 0.001) similarly in both groups, from 3.44 ± 0.55 mmHg ml^{-1} at T60 to 5.36 ± 1.09 mmHg ml^{-1} at T300.

While end-diastolic volume remained unchanged in both groups, coronary reperfusion induced a severe decrease (P < 0.001) in stroke volume SV and in ejection fraction, from 31.0 ± 1.6 ml at T60 to 20.9 ± 2.2 ml at T300, and from 46 ± 2% at T60 to 28 ± 3% at T300, respectively (Fig. 3).

As depicted in Fig. 4, while end-systolic elastance remained statistically unchanged in both groups during reperfusion, dead volume V_d further increased (P< 0.001) from -13.7 ± 3.9 ml at T60 to 9.8 ± 7.7 ml at T300, while left ventriculo-arterial coupling E_{es}/E_a decreased from 0.56 ± 0.11 to 0.43 ± 0.05 (P = 0.01) in the same interval.

During reperfusion, stroke work and pressure-volume area decreased from 2829 ± 244 mmHg ml to 2169 ± 192 mmHg ml (P = 0.02), and from 5616 ± 606 mmHg ml to 4103 ± 563 mmHg ml (P = 0.005), respectively, while mechanical efficiency was statistically unchanged (Fig. 5).

3.2. Macroscopy: risk area and infarct size

Areas at risk in the vehicle-treated group and BM-573-treated group were not different from each other. The area at risk was 33.2 ± 3.4% of left ventricle (LV). In non-treated and BM-573-treated groups, the infarct size, expressed as the percentage of left ventricle was 33.6 ±4.1% and 27.3 ± 2.6% of LV, respectively, or 82% of the area at risk in the BM-573-treated group (Fig. 6A and B). Although the infarct size evidenced by TTC staining was slightly smaller in the treated group, this difference was however not statistically significant (P = 0.32).

Fig. 2: *Evolution of three-element windkessel model parameters during myocardial ischemia and reperfusion. Ischemia was induced immediately after baseline recordings (TO) by occluding the LAD coronary artery, which was reperfused after T60 measurements. R\, characteristic impedance; R_2, peripheral resistance; C, compliance; E_a, effective arterial elastance. *P < 0.05 vs. T0; **P < 0.01 vs. T0; ***P < 0.001 vs. T0; # P < 0.05 vs. T60; ## P<0.01 vs. T60.*

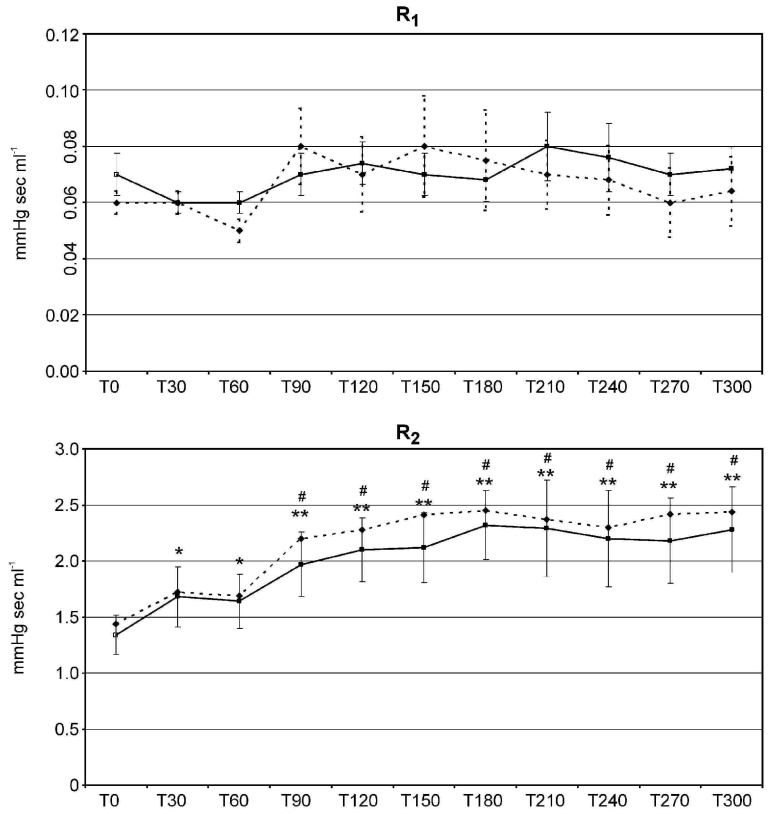

Fig. 2: *(Continued).*

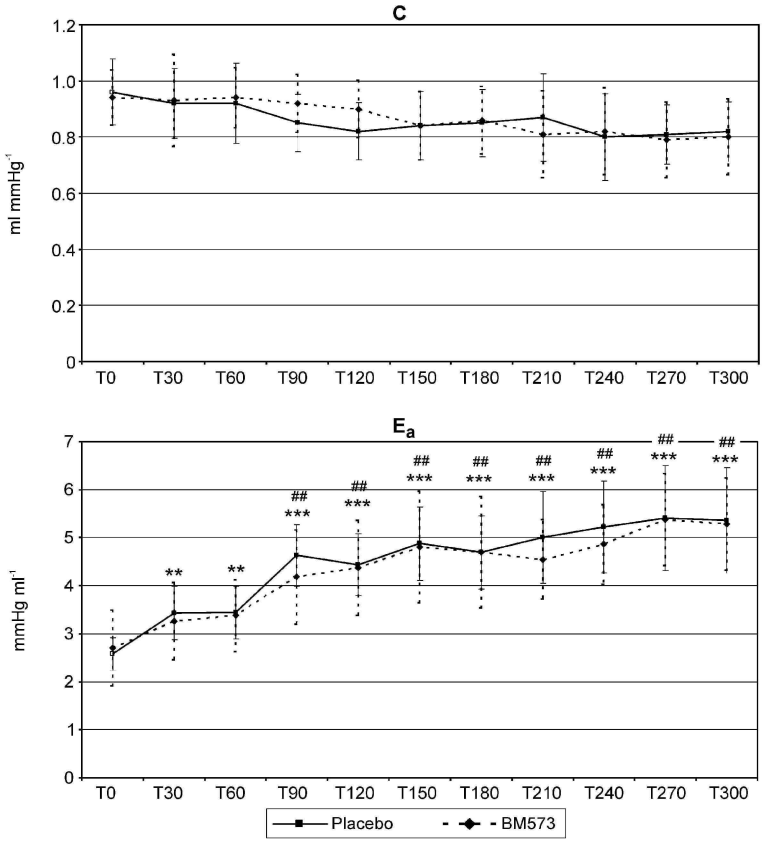

3.3. Histopathology

All hearts from control and BM-573-treated groups were examined by light microscopy. Histopathological examination revealed that main ischemic changes were observed in the anterior left ventricle, corresponding to the area supplied by the LAD coronary artery. Whatever the treatment (vehicle or BM-573), infarcted myocardium displayed altered muscle cells showing a waviness aspect which express prominent myofibrillar contraction bands, anisokaryosis, and accumulation of interstitially infiltrated inflammatory cells as neutrophils and lymphocytes (Fig. 7A). These characteristics also associated with extensive hemorrhage region suggest that these cells probably reached the stage of necrosis. Immunohistochemical detection of desmin revealed, mainly in the anteroseptal region, clear zones of patchy necrosis (Fig. 7D) and blurred zones where it was difficult to clearly delineate necrotic zone from healthy myocardium due to motley aspect (Fig. 7C). Area not supplied by the LAD artery (posterior region) showed normal morphology (Fig. 7B).

3.4. Electron microscopy

Transmission electron microscopy of representative samples was used to characterise myocardium damage and to give a definitive diagnosis. It appeared that whatever the treatment with vehicle or BM-573 (10 mg kg^{-1} h^{-1}), all samples taken in posterior (control) region had the ultrastructural features of healthy myocardium. Indeed, sar-colemma was intact, nuclear chromatin, nucleus and mitochondria were normal (Fig. 8A and B). In vehicle-treated group, all samples from the anteroseptal region (ischemic region) presented irreversible injury characterised by mitochondrial swelling, mitochondria exhibiting amorphous matrix flocculent densities (AMD) or "woolly densities", marked nuclear changes with chromatin clumping, damage to the sarcolemma and breakdown of myofibrillar organisation (Fig. 8C and D). Samples taken in the anteroseptal region from BM-573-treated group showed similar ultrastructural features as those observed in the same region from samples of vehicle-treated group (Fig. 8E and F).

Fig. 3: *Evolution of end-systolic volume V_{es}, end-diastolic volume V_{ed}, stroke volume SV, and ejection fraction EF during myocardial ischemia and reperfusion. Ischemia was induced immediately after baseline recordings (T0) by occluding the LAD coronary artery, which was reperfused after T60 measurements. * P<0.05 vs. T0; ** P<0.01 vs. T0; *** P<0.001 vs. T0; ### P< 0.001 vs. T60.*

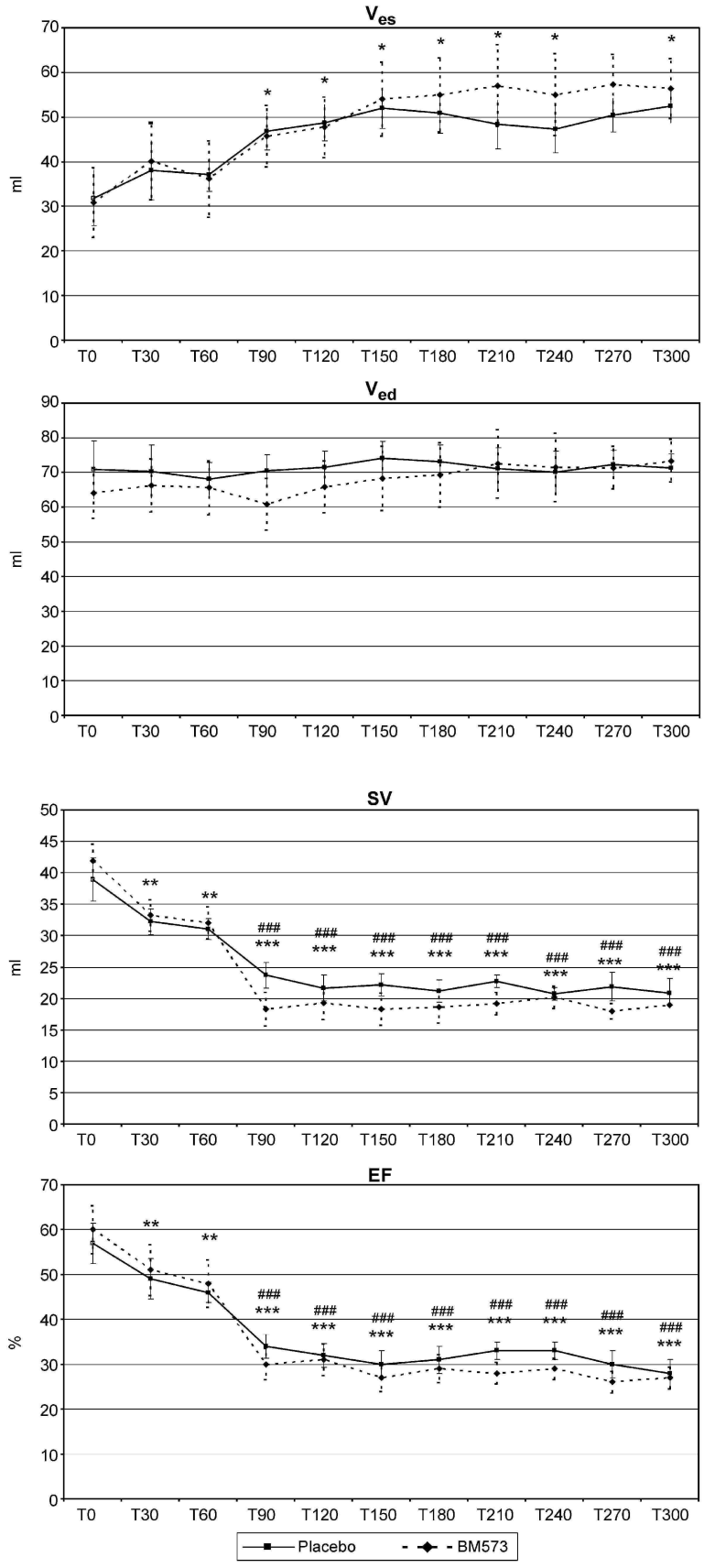

Fig. 4: *Evolution of end-systolic elastance E_{es}, dead volume V_d, slope of PRSW relationship, and ventriculo-arterial coupling E_{es}/E_a during myocardial ischemia and reperfusion. Ischemia was induced immediately after baseline recordings (TO) by occluding the LAD coronary artery, which was reperfused after T60 measurements. PRSW, preload recruitable stroke work. * P<0.05 vs. T0; ** P<0.01 vs. T0; *** P<0.001 vs. T0; # P<0.05 vs. T60; ### P< 0.001 vs. T60.*

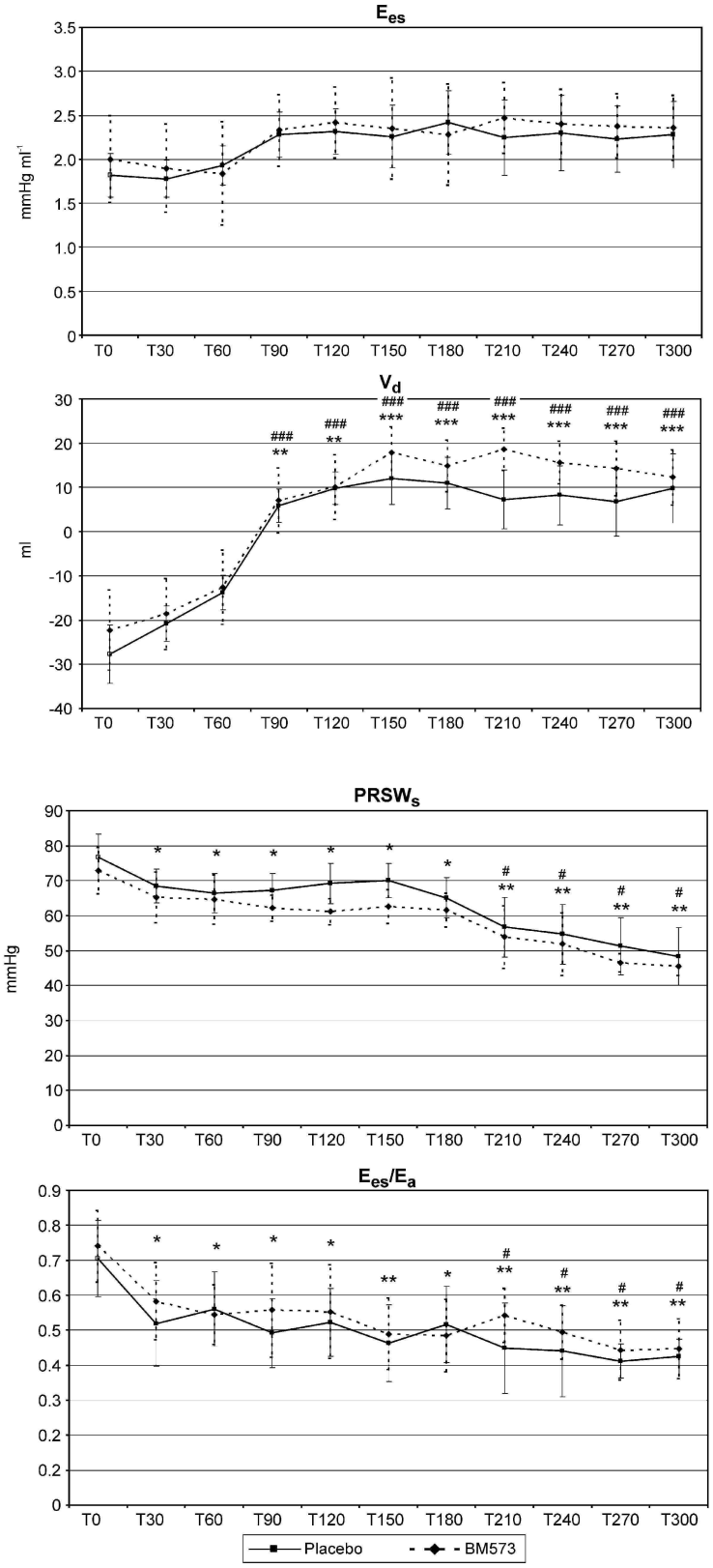

Fig. 5: *Evolution of stroke work SW, pressure-volume area PVA, and mechanical efficiency SW/PVA during myocardial ischemia and reperfusion. Ischemia was induced immediately after baseline recordings (TO) by occluding the LAD coronary artery, which was reperfused after T60 measurements. * P<0.05 vs. T0; ** P<0.01 vs. T0; *** P<0.001 vs. T0; # P<0.05 vs. T60; ## P<0.01 vs. T60.*

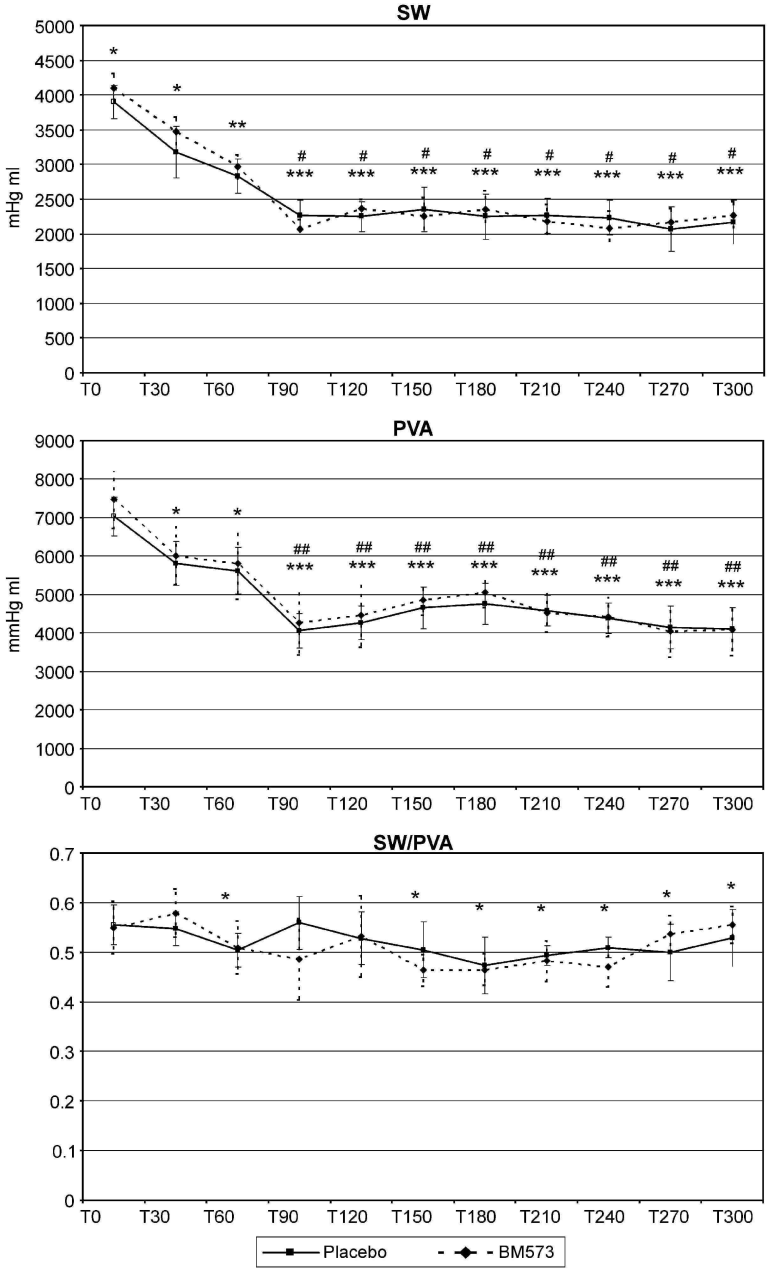

3.5. Biochemical data

ATP content was measured in myocardium from control and BM-573-treated animals. Two samples were judiciously taken from slice two of four hearts in each group, one in the anteroseptal region and one in the posterior region stained by TTC (Fig. 9). In both groups, a significant myocardial ATP decrease was observed in the anteroseptal region compared with the healthy region (posterior) (23540 ± 3328 nmol g^{-1} versus 1384 ± 672 nmol g^{-1} of protein in BM-573-treated pigs and 9844 ± 3880 nmol g^{-1} versus 1330 ± 367 nmol g^{-1} of protein in vehicle-treated pigs). Reperfusion and BM-573 administered during reperfusion failed to prevent drop of ATP or restore the ATP concentration in the anteroseptal region.

A marked elevation of plasma CPK and TnT concentrations were observed in both groups after reperfusion. Data on the graph (Fig. 10A and B) show that BM-573 failed to reduce CPK and TnT plasmatic concentrations.

3.6. Aggregometric data

Platelet aggregation amplitude was evaluated in BM-573 and vehicle groups. In both groups, ex vivo platelet aggregation induced by arachidonic acid or by U-44619 was complete and irreversible at TO. Intravenous infusion (10 mg kg^{-1} h^{-1}) of BM-573 resulted in a complete inhibition of platelet aggregation provoked by arachidonic acid or by U-44619 at T60, T120, T240 and T300. In the vehicle group, platelet aggregation induced by either inducer remained complete and irreversible throughout the experiment (Fig. 11).

4. Discussion

Occlusion of the LAD coronary artery induced a rightward shift of the end-systolic pressure-volume relationship, a decrease in ejection fraction, in cardiac output, in the slope of the SW-EDV relationship, and in mechanical efficiency. All these changes were consistent with an impairment in cardiac performance and efficiency, and matched previous experimental studies on regional myocardial ischemia [33,34]. Furthermore, LV afterload was increased, as evidenced by an augmentation in effective arterial elastance, mainly due to peripheral vasoconstriction, and induced left ventriculo-arterial mismatch. BM-573-treated animals displayed changes in hemodynamic parameters that were similar to those observed in the vehicle group.

In both groups, coronary reperfusion was associated with a further decrease in cardiac performance, as expressed by a drop in cardiac output and in ejection fraction, and a further ESPVR rightward shift. Facing further increased arterial elastance, ventriculo-arterial coupling continued to deteriorate. The impairment in hemodynamic parameters associated with coronary reperfusion was not prevented by BM-573 infusion.

Myocardial infarction was outlined by incubating the heart slices in a buffered solution of TTC, which is reduced to a brick red formazan by dehydrogenase enzymes contained in healthy myocardium. Following necrosis, lack of these enzymes results as an unstained area. After 60 min of occlusion followed by 4 h of reperfusion, the percent of infarct area was similar to that of the area at risk, and histologic changes, mainly located in the anteroseptal region, were not ameliorated by BM-573 administration. Furthermore, increased plasma concentrations of CPK and TnT, indicators of tissue necrosis, were not reduced and similar drops of ATP level, measured in anteroseptal region versus posterior region, were observed in the vehicle group and in the BM-573-treated group.

Thromboxane A_2 is a major prostanoid in the cardiovascular system, whose biological properties include platelet aggregation, constriction of vascular smooth muscles, and leukocyte chemotaxis [35]. In the vascular system, TXA_2 is produced mainly by platelets, but it has also been found to be produced by cardiomyocytes, suggesting some direct role in the heart. Moreover, its synthesis is significantly increased during ischemia-reperfusion [13,14,36], and its rhodopsin-type receptor, TP, has been reported to be expressed on cardiomyocytes [37].

Several studies have reported the beneficial effects of TXA_2 synthase inhibitors on cardiac ischemia-reperfusion [17,38-40]. Such beneficial effects were, at least partly, attributed to enhanced generation of PGI2 derived from increased availability of its precursor, resulting in inhibition of neutrophil adhesion to endothelial cells [17,39].

In contrast, studies evaluating the effects of TXA2 antagonists during myocardial ischemia-reperfusion yielded contradictory results. Indeed, beneficial effects of TP antagonists in cardiac ischemia-reperfusion have been reported in several studies in dogs [15], in cats [16,41,42] and in rats [43]. However, others have not observed such a protective effect [17,18].

Recently, Ge et al. [18] compared two TXA_2 receptor antagonists, KT2-962 and daltroban (BM 13.505) in an open-chest dog model of myocardial ischemia-reperfusion injury. They found that administration of KT2-962, but not daltroban, significantly reduced the incidence of ventricular fibrillation during the ischemic period and the myocardial area at risk by about 40%. They subsequently showed, using electron spin resonance spectroscopy, that KT2-962 inhibited the formation of hydroxyl radicals, whereas daltroban had no effect. These authors concluded that the beneficial effects of KT2-962 was probably due to its direct free radical scavenging properties rather than its ability to block TXA_2 receptors.

Among several factors that may contribute to such discrepancy, are differences in animal species, degree of collateral blood flow, duration of ischemia, timing of drug administration, drug delivery method, and different end-points of cardio protection (infarct size, myocardial function, endothelial function or arrhythmias). Another factor may result from the fact that some TP antagonists, but not others, cross-act on other prostanoid receptors, such as EP3, through which PGE2 was reported to exert protective effects on cardiac ischemia-reperfusion injury

[44].

Concerning animal species, numerous studies have used a canine or a feline model. However, the use of dogs or cats in the setting of myocardial ischemia-reperfusion has some important pathophysiological drawbacks, such as the often substantial and unpredictable coronary collateral blood flow in these species. Pigs were used in this study because of the similarity between hearts from pigs and humans concerning the physiological properties, the anatomical distribution of coronary arteries, the lack of collateral circulation and the heart-to-body weight ratio [45,46].

Duration of ischemia in another factor of importance. In pigs, Miyazaki et al. [47] studied the effects of various duration (20, 30, 60 and 120 min) of LAD coronary artery occlusion followed by 8 h of reperfusion. With an occlusion time of 60 min, they found results similar to ours. Actually, they showed a transmural infarct despite reperfusion after 60 min of occlusion. They observed that the infarct area after reperfusion increased significantly with the duration of the occlusion and reached 80 ± 9% of the risk area when the LAD was occluded during 60 min. Other studies demonstrated that 1 h of ischemia (without reperfusion) was sufficient to produce severe myocardial lesions, because of absence of collateral circulation in pig heart [48].

After 4 h of reperfusion and despite associated BM-573 infusion, major structural changes were caused in myocytes. Thus, myocardial ATP content did not recover and electron microscopy showed irreversible injury notably characterised by appearance of mitochondrial amorphous matrix (flocculent) densities (AMD) which are complexes of insoluble proteins and lipid resulting from destruction of mitochondrial membranes [49,50].

Fig. 6: *Photographs of gross slices of heart after TTC staining from vehicle-treated animals suffering from 1 h of ischemia and 4 h of reperfusion (A), and from BM-573-treated animals suffering from 1 h of ischemia and 4 h of reperfusion (B).*

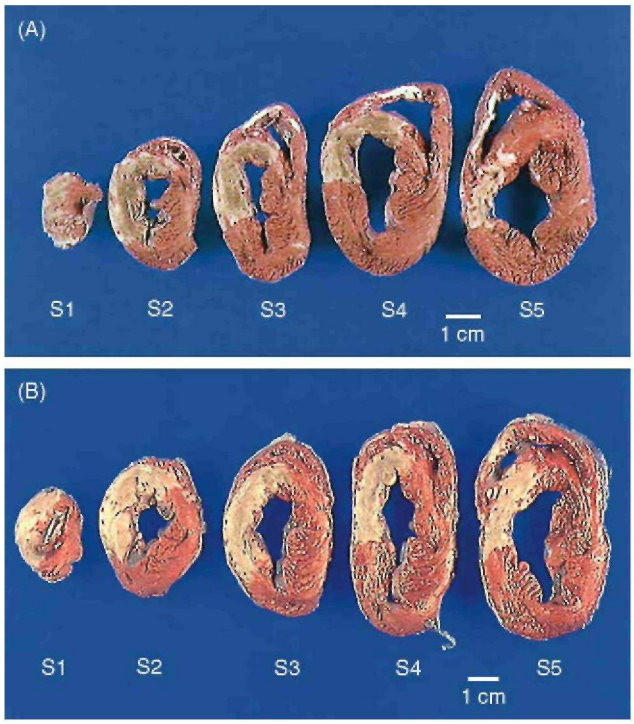

Fig. 7: *Light micrographs of myocardial necrosis occurring during ischemia (1 h) and 4 h of reperfusion, without and with BM-573 treatment. (A) Wavy aspect of the necrotic fibres and accumulation of interstitially infiltrated inflammatory cells in anteroseptal region of control pig (Masson's trichrome stain, original magnification × 200). (B-D) Immunohistological staining of desmin. Normal myocardial muscle in the posterior region (B, original magnification × 400). Motley aspect of myocardium in the anteroseptal region of BM-573-treated pig where separation between necrotic and viable myocardium is not obvious (C, original magnification × 200). Patchy necrosis is shown at the lower right portion of the photomicrograph (arrow) taken in anteroseptal region of control pig (D, original magnification × 100).*

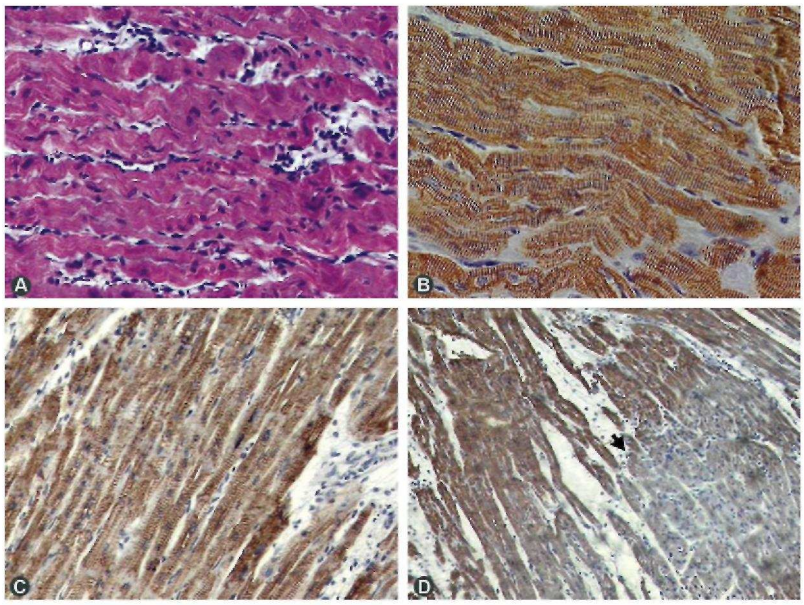

In this study, BM-573 was administered intravenously at the dose of 10 mg kg^{-1} h^{-1}. This was sufficient to prevent platelet aggregation induced by arachidonic acid suggesting that the thromboxane receptors are blocked. Moreover, in a previous study, our team demonstrated that this regimen was also responsible for a complete inhibition of the thromboxane synthase revealed by a prevention of TXA_2 overproduction. These results confirm the efficacy of BM-573 as a potent TXA_2 receptor antagonist [20,21], indicating that, although the drug was ineffective in this ischemia-reperfusion model, it remains active as thromboxane modulator.

However, it could be argued that this route of administration may be insufficient during myocardial ischemia, essentially because the drug did not reach the ischemic area in the absence of collateral circulation. Further, intravenous administration usually requires a large dose in order to achieve adequate concentration in the ischemic -reperfused area. Accordingly, a substantial amount of the substance reaches the non-ischemic area with possible risk of negative impact on myocardial function. In addition, systemic effects can also be observed, for example by modifying systemic vascular resistances that in turn cause changes in cardiac afterload and subsequently in the infarct size.

Other possible routes for drug administration include antegrade arterial intracoronary perfusion, which may however interfere with coronary blood flow, and coronary venous retroperfusion. Ryden et al. [51] have shown that coronary venous retroperfusion led to the accumulation of substantial amounts of drug specifically in the ischemic parts of the myocardium, while concentrations in plasma and in non-ischemic myocardium remained low. We chose to use the intravenous route because it is closer to the clinical setting. Further, we have previously shown that BM-573 has no direct effect on cardiac function nor on vascular afterload [20]. However, it is possible that administration of BM-573 through the coronary venous retroperfusion route would have yielded different results.

In a recent study, Xiao et al. [52] assessed the roles of prostaglandin I_2 and TXA_2 in cardiac ischemia-reperfusion injury, using mice lacking their respective receptors. While they demonstrated that PGI_2, produced endogenously during myocardial ischemia-reperfusion, exerts a protective effect on cardiomyocytes, these authors concluded that TXA_2 has little role in cardiac ischemia-reperfusion injury.

Fig. 8: *Ultrastructure of normal myocardium (posterior region) with normal mitochondria, nucleus presenting normal chromatin (A) and intact sarcolemma (B). Irreversibly injured myocardium with mitochondrial swelling (C, D and F) presenting amorphous matrix densities (AMD), distortion of sarcomeres and contraction bands (D and E), and chromatin clumping (E). A (×10,000) and B (×8000) were taken from samples of posterior region from a vehicle-treated pig. (C) (×20,000) and (D) (×12,000) were taken from samples of anteroseptal region from a vehicle-treated pig. (E) (×6000) and (F) (×10,000) were taken from samples of anteroseptal region from a BM-573-treated pig.*

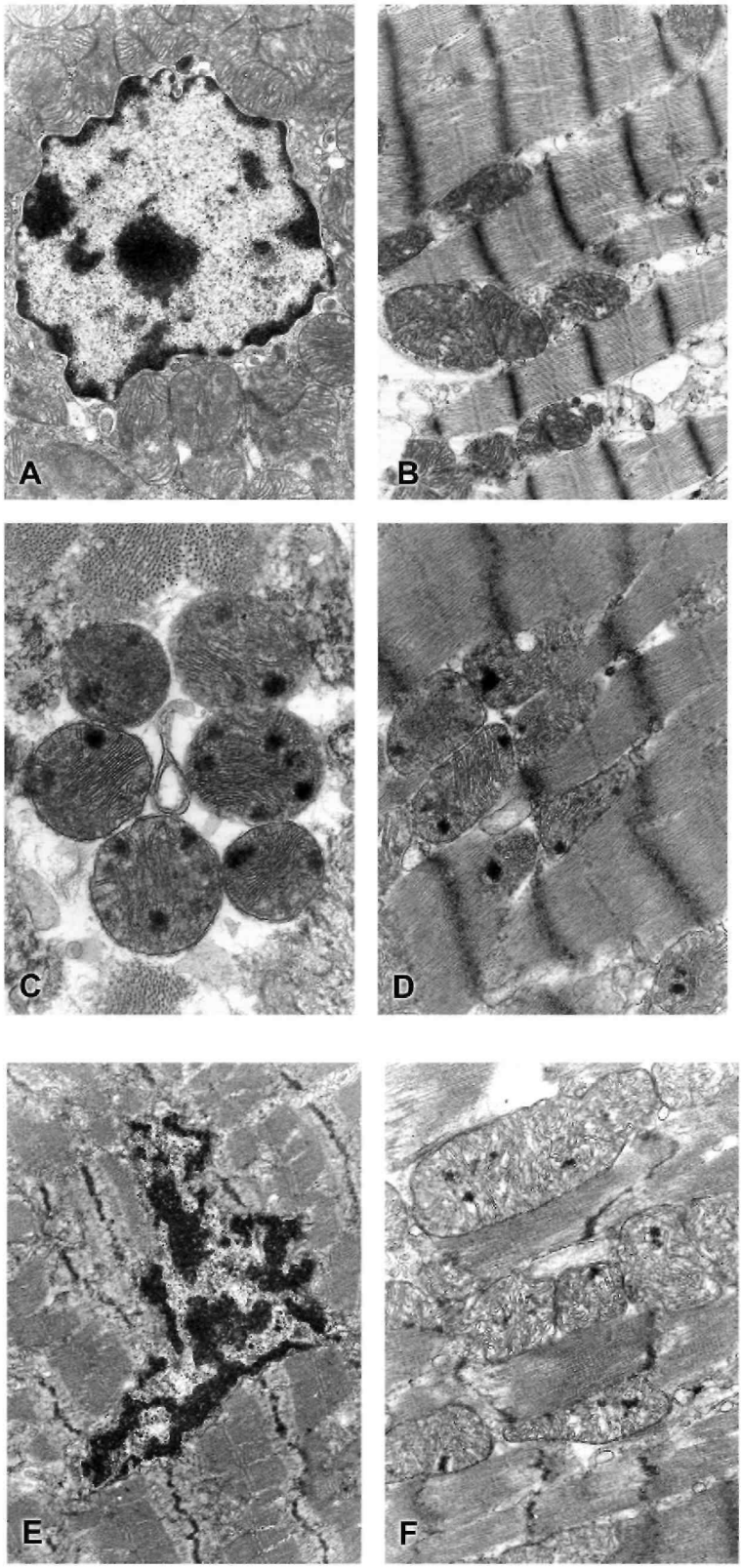

Fig. 9: *ATP content (nanomoles per gram of protein) of heart slice two from control animals (n = 4) and BM-573-treated animals (n = 4) (*** P < 0.001 and * P<0.5).*

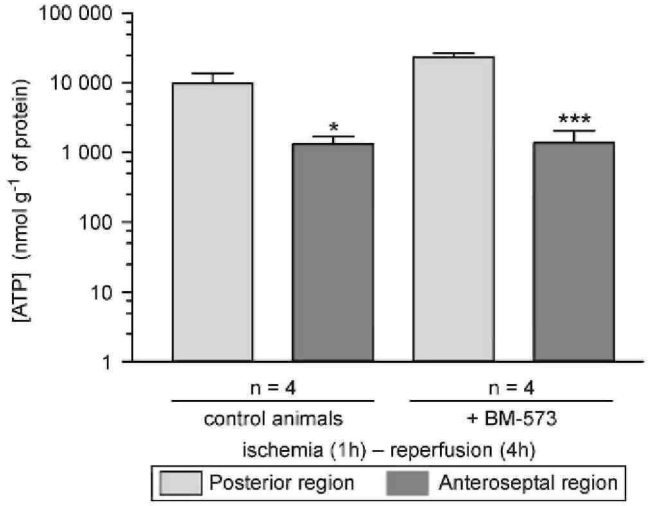

Fig. 10: *Effect of BM-573 (A) on plasma creatine phosphokinase (CPK) concentration in international unit ($IU1^{-1}$) and (B) on plasma troponine T (TnT) concentration ($\mu g l^{-1}$).*

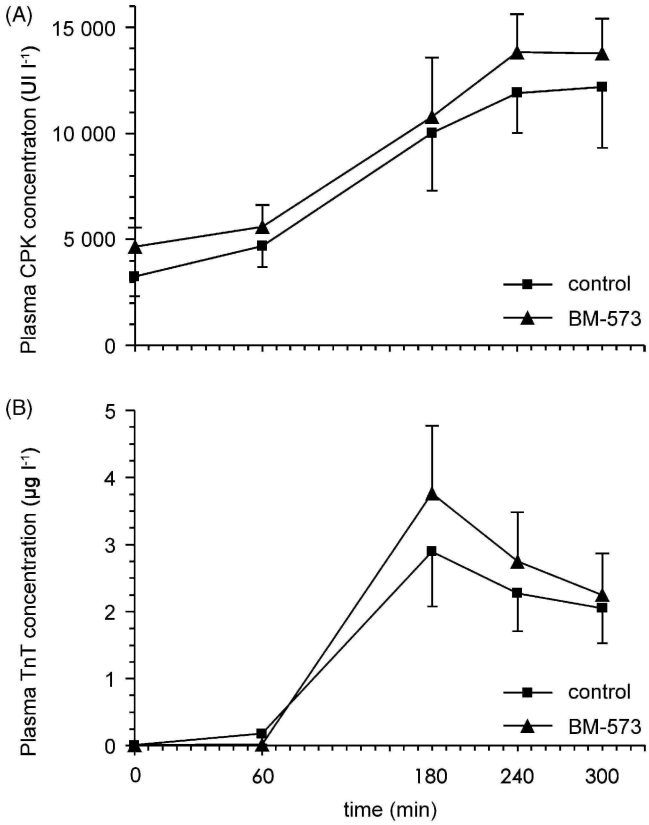

However, the actions of TXA_2 on platelets and vasculature should contribute to the pathogenesis of atherosclerosis and/or vasospasm, prerequisites for coronary artery disease. Recently, we showed, in a porcine model, that BM-573 was able to prevent the formation of an occlusive thrombus in $FeCl_3$ -induced endothelium-damaged LAD coronary artery, and the development of subsequent myocardial infarction [20]. This $FeCl_3$ model, as compared to direct occlusion, mimics more closely the development of an occlusive thrombus at the site of a ruptured atherosclerotic plaque in humans, but cannot be used to study myocardial ischemia-reperfusion

as it triggers irreversible endothelial lesions.

Fig. 11: *Time course of platelet aggregation amplitude induced by arachidonic acid in the vehicle group (black columns) and in the BM-573 group (empty columns).*

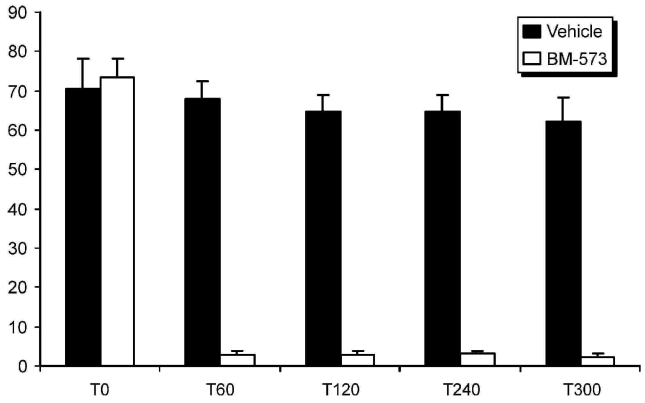

Conclusion

In conclusion, this study showed that BM-573, a combined TXA_2 synthesis inhibitor and receptor antagonist, failed, at macroscopic, histopathological, and ultrastructural levels, to reduce the extension of myocardial tissue damage in a porcine model of ischemia-reperfusion. Biochemical and hemodynamic analysis confirmed the installation of a severe myocardial infarction despite BM-573 administration.

However, as one of the most important mediator triggering platelet aggregation, TXA_2 participates in coronary artery thrombus formation which potentially leads to acute myocardial infarction and severe tissue damage. Consequently, prevention of myocardial infarction remains a major indication for the use of a thromboxane modulator, such as BM-573, as demonstrated by our team in a previous study [20]. This indeed supports the mode of action and the efficacy of aspirin in prevention of acute thrombotic events.

Acknowledgments

This research was supported by grants from the ARC 94/99-177 of the Communauté Française de Belgique, from the Belgian National Fund for Scientific Research, and from the Leon Fredericq Foundation of the University of Liege. Philippe Kolh and Vincent Tchana-Sato are funded, respectively, by a post-doctoral grant and by a doctoral grant of the National Fund for Scientific Research, Belgium.

The authors gratefully thank Dr. Michaela Oana for advice on this experiment, Dr. Carine Michiels for help with ATP dosage, Mrs. Cécile Meraglia and Mr. Luc Leroy for excellent technical assistance in histology and electronic microscopy, respectively.

References

[1] GISSI Investigators. Effectiveness of intravenous thrombolytic treatment in acute myocardial infarction. Gruppo Italiano per lo Studio della Streptochinasi nell'Infarto Miocardico (GISSI). Lancet 1986;1:397.

[2] Grines CL, Browne KF, Marco J, et al. A comparison of immediate angioplasty with thrombolytic therapy for acute myocardial infarction. The Primary Angioplasty in Myocardial Infarction Study Group. N Engl J Med 1993;328:673.

[3] Zijlstra F, de Boer MJ, Hoorntje JC, Reiffers S, Reiber JH, Suryapranata H. A comparison of immediate coronary angioplasty with intravenous streptokinase in acute myocardial infarction. N Engl J Med 1993;328:680.

[4] GUSTO Investigators. An international randomized trial comparing four thrombolytic strategies for acute myocardial infarction. The GUSTO investigators. N Engl J Med 1993;329:673.

[5] Hearse DJ, Humphrey SM, Nayler WG, Slade A, Border D. Ultrastructural damage associated with reoxygenation of the anoxic myocardium. J Mol Cell Cardiol 1975;7:315.

[6] Opie LH. Reperfusion injury and its pharmacologic modification. Circulation 1989;80:1049.

[7] Reimer KA, Tanaka M, Murry CE, Richard VJ, Jennings RB. Evaluation of free radical injury in myocardium. Toxicol Pathol 1990;18:470.

[8] Haga Y, Hatori N, Nordlander M, Nordlander R, Sjoquist PO, Ryden L. Coronary venous retroinfusion of felodipine reducing infarct size without affecting regional myocardial blood flow. Eur Heart J 1993;14:1386.

[9] Hatori N, Haga Y, Sjoquist PO, Nordlander M, Ryden L. Coronary venous retroinfusion of felodipine reduces myocardial necrosis after coronary occlusion and reperfusion. J Cardiovasc Pharmacol 1993;22:160.

[10] Wang QD, Li XS, Lundberg JM, Pernow J. Protective effects of non-peptide endothelin receptor antagonist bosentan on myocardial ischaemic and reperfusion injury in the pig. Cardiovasc Res 1995;29:805.

[11] Fitzgerald DJ, Roy L, Catella F, FitzGerald GA. Platelet activation in unstable coronary disease. N Engl J Med 1986;315:983.

[12] Tada M, Kuzuya T, Hoshida S, Nishida M. Arachidonate metabolism in myocardial ischemia and reperfusion. J Mol Cell Cardiol 1988;20(Suppl.2):135.

[13] Tanabe M, Terashita ZI, Fujiwara S, et al. Coronary circulatory failure and thromboxane A2 release during coronary occlusion and reperfusion in anaesthetised dogs. Cardiovasc Res 1982;16:99.

[14] Kuzuya T, Hoshida S, Nishida M, Kim Y, Kamada T, Tada M. Increased production of arachidonate metabolites in an occlusion-reperfusion model of canine myocardial infarction. Cardiovasc Res 1987;21:551.

[15] Higo K, Sano J, Karasawa A, Kubo K. The novel thromboxane A2 receptor antagonist KW-3635 reduces infarct size in a canine model of coronary occlusion and reperfusion. Arch Int Pharmacodyn Ther 1993;323:32.

[16] Bhat AM, Sacks H, Osborne JA, Lefer AM. Protective effect of the specific thromboxane receptor antagonist, BM-13505, in reperfusion injury following acute myocardial ischemia in cats. Am Heart J 1989; 117:799.

[17] Golino P, Ambrosio G, Villari B, et al. Endogenous prostaglandin endoperoxides may alter infarct size in the presence of thromboxane synthase inhibition: studies in a rabbit model of coronary artery occlusion-reperfusion. J Am Coll Cardiol 1993;21:493.

[18] Ge ZD, Auchampach JA, Piper GM, Gross GJ. Comparison of cardioprotective efficacy of two thromboxane A2 receptor antagonists. J Cardiovasc Pharmacol 2003 ;41:481.

[19] Rolin S, Dogne JM, Michaux C, Delarge J, Masereel B. Activity of a novel dual thromboxane A(2)receptor antagonist and thromboxane synthase inhibitor (BM-573) on platelet function and isolated smooth muscles. Prostaglandins Leukot Essent Fatty Acids 2001 ;65:67.

[20] Rolin S, Petein M, Tchana-Sato V, et al. BM-573, a dual thromboxane synthase inhibitor and thromboxane receptor antagonist, prevents pig myocardial infarction induced by coronary thrombosis. J Pharmacol Exp Ther 2003;306:59.

[21] Dogne JM, Hanson J, de Levai X, et al. Pharmacological characterization of *N-tert*-butyl-*N'*-[2-(4'-methylphenylamino)-5-nitrobenzenesulfonyl]urea (BM-573), a novel thromboxane A2 receptor antagonist and thromboxane synthase inhibitor in a rat model of arterial thrombosis and its effects on bleeding time. J Pharmacol Exp Ther 2004;309:498.

[22] Baan J, van der Velde ET, De Bruin HG, et al. Continuous measurement of left ventricular volume in animals and humans by conductance catheter. Circulation 1984;70:812.

[23] Suga H, Kitabatake A, Sagawa K. End-systolic pressure determines stroke volume from fixed end-diastolic volume in the isolated canine left ventricle under a constant contractile state. Circ Res 1979;44:238.

[24] Suga H. External mechanical work from relaxing ventricle. Am J Physiol 1979;236:H494 (Heart Circ Physiol 5).

[25] Denslow S. Relationship between PVA and myocardial oxygen consumption can be derived from thermodynamics. Am J Physiol 1996;270:H730 (Heart Circ Physiol 39).

[26] Westerhof N, Elzinga G, Sipkema P. An artificial arterial system for pumping hearts. J Appl Physiol 1971;31:776.

[27] Lambermont B, Kolh P, Detry O, Gerard P, Marcelle R, D' Orio V. Analysis of endotoxin effects on the intact pulmonary circulation. Cardiovasc Res 1999;41:275.

[28] Sagawa K, Maughan L, Suga H, Sunagawa K, editors. Cardiac contraction and the pressure-volume relationship. New York: Oxford University Press; 1988.

[29] Warltier DC, Zyvoloski MG, Gross GJ, Hardman HF, Brooks HL. Determination of experimental myocardial infarct size. J Pharmacol Methods 1981;6:199.

[30] Higo K, Karasawa A, Kubo K. Early thrombolysis by recombinant tissue-plasminogen activator is beneficial to the ischemic myocardium. J Pharmacobiodyn 1992;15:33.

[31] Lie JT, Pairolero PC, Holley KE, Titus JL. Macroscopic enzyme-mapping verification of large, homogeneous, experimental myocardial infarcts of predictable size and location in dogs. J Thorac Cardiovasc Surg 1975;69:599.

[32] Fishbein MC, Meerbaum S, Rit J, et al. Early phase acute myocardial infarct size quantification: validation of the triphenyl tetrazolium chloride tissue enzyme staining technique. Am Heart J 1981;101:593.

[33] Sunagawa K, Maughan WL, Sagawa K, et al. Effect of regional ischemia on the left ventricular end-systolic pressure-volume relationship of isolated canine hearts. Circ Res 1983;52:170.

[34] Kass DA, Marino P, Maughan W, Sagawa K. Determinants of end-systolic pressure-volume relations during acute regional ischemia in situ. Circulation 1989;80:1783.

[35] Coleman R, Kennedy I, Humphrey P. Comprehensive medicinal chemistry vol. 3: membranes and receptors. In: Emmett J, editor. Prostanoids and their receptors. Oxford, UK: Pergamon Press; 1990. p.643.

[36] Coker SJ, Parratt JR, Ledingham IM, Zeitlin IJ. Thromboxane and prostacyclin release from ischaemic myocardium in relation to arrhythmias. Nature 1981;291:323.

[37] Bowling N, Dube GP, Kurtz WL, et al. Characterization of thromboxane A2/prostaglandin H2 binding sites in guinea pig cardiac membrane preparations. J Mol Cell Cardiol 1994;26:915.

[38] Imamoto T, Terashita Z, Tanabe M, Nishikawa K, Hirata M. Protective effect of a novel thromboxane synthetase inhibitor, CV-4151, on myocardial damage due to coronary occlusion and reperfusion in the hearts of anesthetized dogs. J Cardiovasc Pharmacol 1986;8:832.

[39] Mullane KM, Fornabaio D. Thromboxane synthetase inhibitors reduce infarct size by a platelet-dependent, aspirin-sensitive mechanism. Circ Res 1988;62:668.

[40] Nichols WW, Mehta J, Wargovich TJ, Franzini D, Lawson D. Reduced myocardial neutrophil accumulation and infarct size following thromboxane synthetase inhibitor or receptor antagonist. Angiology 1989;40:209.

[41] Schror K, Thiemermann C. Treatment of acute myocardial ischaemia with a selective antagonist of thromboxane receptors (BM 13.177). Br J Pharmacol 1986;87:631.

[42] Brezinski ME, Yanagisawa A, Lefer AM. Cardioprotective actions of specific thromboxane receptor antagonist in acute myocardial ischemia. J Cardiovasc Pharmacol 1987;9:65.

[43] Hock CE, Brezinski ME, Lefer AM. Anti-ischemic actions of a new thromboxane receptor antagonist, SQ-29,548, in acute myocardial ischemia. Eur J Pharmacol 1986;122:213.

[44] Hohlfeld T, Meyer-Kirchrath J, Vogel YC, Schror K. Reduction of infarct size by selective stimulation of prostaglandin EP(3) receptors in the reperfused ischemic pig heart. J Mol Cell Cardiol 2000; 132:285.

[45] White F, Bloor C. Coronary collateral circulation in the pig: correlation of collateral flow with coronary bed size. Basic Res Cardiol 1981 ;76:189.

[46] Schaper W, Gorge G, Winkler B, Schaper J. The collateral circulation of the heart. Prog Cardiovasc Dis 1988;31:57.

[47] Miyazaki S, Fujiwara H, Onodera T, et al. Quantitative analysis of contraction band and coagulation necrosis after ischemia and reperfusion in the porcine heart. Circulation 1987;75:1074.

[48] Taylor IM, Shaikh NA, Downar E. Ultrastructural changes of ischemic injury due to coronary artery occlusion in the porcine heart. J Mol Cell Cardiol 1984; 16:79.

[49] Jennings RB, Ganote CE. Mitochondrial structure and function in acute myocardial ischemic injury. Circ Res 1976;38(Suppl. 1):I80.

[50] Becker LC, Jeremy RW, Schaper J, Schaper W. Ultrastructural assessment of myocardial necrosis occurring during ischemia and 3-h reperfusion in the dog. Am J Physiol 1999;277:H243.

[51] Ryden L, Tadokoro H, Sjoquist PO, et al. Pharmacokinetic analysis of coronary venous retro infusion: a comparison with anterograde coronary artery drug administration using metoprolol as a tracer. J Am Coll Cardiol 1991;18:603.

[52] Xiao CY, Hara A, Yuhki K, et al. Roles of prostaglandin I(2) and thromboxane A(2) in cardiac ischemia-reperfusion injury: a study using mice lacking their respective receptors. Circulation 2001; 104:2210.